available at www.sciencedirect.com

ScienceDirect

journal homepage: www.elsevier.com/locate/cortex

Special issue: Research report

Motor cortical activity related to movement kinematics exhibits local spatial organization

Eran Stark[a,*], *Rotem Drori*[a,b] *and Moshe Abeles*[a,b,c]

[a]*Department of Physiology, Hadassah Medical School, Hebrew University, Jerusalem, Israel*
[b]*Interdisciplinary Center for Neural Computation, Hebrew University, Jerusalem, Israel*
[c]*Gonda Brain Research Center, Bar-Ilan University, Ramat-Gan, Israel*

ARTICLE INFO

Article history:
Received 21 June 2007
Reviewed 16 November 2007
Revised 6 December 2007
Accepted 4 March 2008
Published online 10 July 2008

Keywords:
Motor cortex
Movement
Temporal correlations
Extra-cellular recordings
Macaque monkey

ABSTRACT

While it is generally accepted that multiple neurons cooperate to generate movement, the precise mechanisms are largely unknown. One way to generate a robust local control signal is for nearby neurons to share similar properties. To study this possibility, we recorded neural activity from the macaque motor cortex during two drawing tasks: free scribbling, and tracing given paths. We analyzed neural activity in relation to three kinematic parameters – position, velocity, and acceleration – while explicitly considering temporal correlations between them. Single-unit (SU) activity was typically related to one parameter, most often velocity, and tended to precede movement. Different SUs encoded different parameters, but nearby units tended to prefer the same parameter. Moreover, while SUs covered a wide range of positions, velocity directions, and acceleration directions, SUs recorded by the same electrode tended to prefer similar values of the same parameter. Nevertheless, some nearby units exhibited marked differences. Multi-unit activity (MUA), estimating the spiking activity of many neurons around the recording electrode, also tended to be related to one parameter and precede movement. However, overall correlations between MUA and movement were more than twice as strong as SU correlations. Finally, SUs and MUAs recorded by the same electrode tended to share similar properties. These two lines of evidence converge to suggest that activity of motor cortex neurons within approximately 200 micrometers is accumulated in a manner useful for representing a single parameter. However, even within a small region there are also neurons related to other parameters, potentially facilitating coordination between distinct parameters.

1. Introduction

To understand how drawing movements are generated by humans, we need to understand the brain mechanisms underlying movement. A useful model system for pursuing this goal is the macaque monkey, which can be trained to perform drawing movements. During monkey drawing, extra-cellular neural activity can be recorded from brain regions known to be associated with motor output including the primary motor and premotor cortices (Hatsopoulos et al., 2004; Paninski et al., 2004; Schwartz, 1994; Schwartz et al., 2004; Stark et al., 2007b). In this framework, specific questions

* *Corresponding author*. Department of Physiology, Hadassah Medical School, Hebrew University, Jerusalem 91120, Israel.
E-mail address: eran.stark@ekmd.huji.ac.il (E. Stark).
0010-9452/$ – see front matter © 2008 Elsevier Srl. All rights reserved.
doi:10.1016/j.cortex.2008.03.011

about the relations between neural activity and drawing movements can be formulated and addressed.

One topic which has been addressed repetitively is which and how many movement parameters are represented in neuronal activity. Motor cortical neurons have been related to almost every tested parameter including force (Evarts, 1968), changes in force (Humphrey et al., 1970), muscle activity (Fetz and Cheney, 1980), direction (Georgopoulos et al., 1982), acceleration (Flament and Hore, 1988), arm posture (Kettner et al., 1988), joint torques (Riehle and Requin, 1995), speed (Moran and Schwartz, 1999), changes in joint angles (Reina et al., 2001), and joint angles (Aflalo and Graziano, 2006). Several studies have even suggested that a single neuron is related to multiple parameters (Ashe and Georgopoulos, 1994; Fu et al., 1995; Paninski et al., 2004). This has led to the proposition that single neurons might not represent a fixed parameter (Fetz, 1992). However, the study of relations between neural activity and movement parameters is inherently complicated by correlations between parameters measured in different coordinate frames (Todorov, 2000) or at different times (Stark et al., 2006). For instance, to touch a target the hand must move there, resulting in temporal correlations between hand position and velocity direction.

A related issue is whether and how multiple neurons cooperate to generate movement. One possible means of cooperation is for nearby neurons to form functional groups that share similar properties, yielding a robust local control signal. While the concept of cortical columns is well-established for sensory cortices (somatosensory cortex: Mountcastle, 1957; visual cortex: Hubel and Wiesel, 1962; auditory cortex: Imig and Adrian, 1977), there is little published evidence on the spatial organization of movement parameters in the motor cortex. Recently, however, it was shown that nearby motor cortical neurons tend to prefer similar reach directions (Ben-Shaul et al., 2003; Georgopoulos et al., 2007), specifically when recorded from arm-related, but not finger-related, sites (Stark et al., 2007a). However, these results were obtained using center-out tasks and analysis methods that did not account for temporal correlations between parameters. Thus, it is unclear whether the observed similarities between nearby neurons reflect similar preferred positions, similar velocity preferred directions (PDs), similar acceleration PDs, temporal correlations between these parameters, or other factors.

Here, we address these issues using the macaque drawing model system while explicitly considering temporal correlations between parameters. From a behavioral perspective we focus on drawing kinematics: end-point position, velocity, and acceleration. From the neural perspective, we examine activity of well-isolated single-units (SUs) and multi-unit activity (MUA) which is used as an estimate of the superimposed activity of many neurons around the recording electrode.

2. Methods

2.1. *Animals and behavioral tasks*

Two monkeys (female *Macaca fascicularis*, U/F, 3/3.5 kg) were used in this study. Animal handling procedures were in accordance with the NIH Guide for the Care and Use of Laboratory Animals (1996), complied with Israeli law, and approved by the Ethics Committee of the Hebrew University. Monkeys were trained to sit in a primate chair and to perform drawing movements with their preferred hand (U/F: right/left) by operating a two-joint low-friction planar manipulandum. A horizontal opaque screen, mounted at chest level, blocked view of the manipulandum and hand, and on this screen a circular cursor indicating hand end-point was projected (Fig. 1, yellow dots). The behavioral tasks were described elsewhere (Stark et al., 2007b) and are briefly summarized below.

In the scribbling task (Fig. 1A) only the cursor was visible. When the monkey moved the cursor into an invisible hexagon a trial was considered successful and the monkey was rewarded by a drop of juice. Immediately another hexagon was randomly selected and the process repeated. The monkey performing this task (U) completed 689 scribbles per session (median; range: 499–1076, 18 sessions), each 1.3 sec long (median; 95% range: .1–5.8 sec).

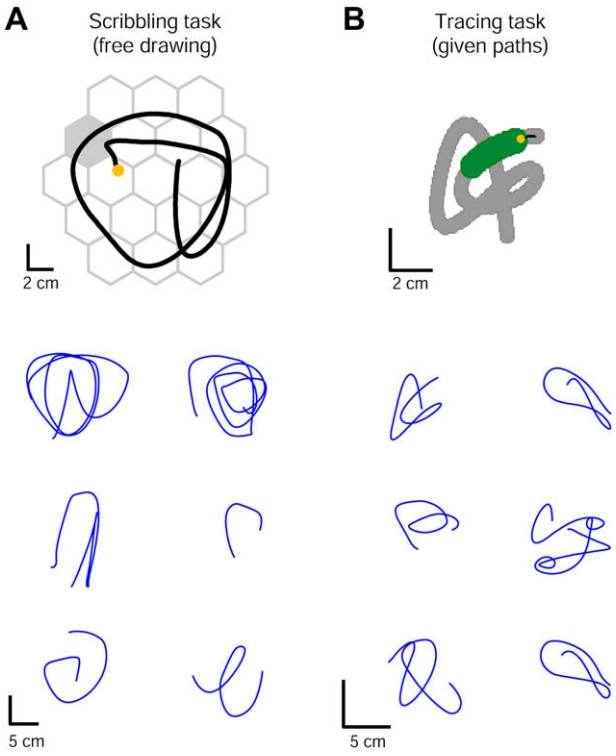

Fig. 1 – Drawing tasks. During both tasks monkeys moved a two-joint manipulandum in the horizontal plane and saw a circular cursor indicating hand end-point (yellow dot). (A) *Top panel*: scribbling task. In this task the monkey saw only the cursor. Once an invisible target (gray hexagon) was entered the monkey was rewarded, and then another target was randomly selected and the process was repeated. *Bottom panels*: examples of actual monkey scribbles. (B) *Top panel*: tracing task. In each trial a randomly selected path was shown in gray. As the monkey moved the yellow cursor along the path, the green marker was advanced indicating the immediate path the monkey had to follow. *Bottom panels*: examples of traced paths.

In the tracing task (Fig. 1B) the monkey traced given paths at its own pace. During each session 40 different paths were used, each generated by fitting a cubic spline to 10 randomly-chosen points and consisting of 64–125 points (median: 90). At the beginning of a trial, one path was randomly selected and its origin was displayed as a green circle. After the money placed the cursor inside the origin, the entire path was shown as partially overlapping gray circles. The first eight circles were colored green. As the monkey moved the cursor into the first green circle, the circle changed color to gray and the subsequent gray circle in the path turned green, a process that was repeated until the entire path was traced. A trial was considered successful and the monkey was rewarded if the entire path was traced without pausing for more than 800 msec between successive circles; otherwise, the trial was aborted. The monkey performing this task (F) completed 334 tracing trials per session (median of 22 sessions; range: 218–487), each 3.4 sec long (median; 95% range: 2–5.9 sec).

2.2. *Recording procedures*

During each recording session up to eight glass-coated tungsten microelectrodes (impedance .2–1.5 MΩ at 1 kHz) confined to a guide tube (internal diameter 1.5 mm) were inserted into arm-related regions of the primary motor cortex (M1) or the dorsal premotor cortex (PMd) contra-lateral to the preferred hand using a computer-controlled microdrive (electrode positioning system (EPS), Alpha-Omega Engineering, Nazareth, Israel). Arm relations were assessed by passive limb manipulations and by intra-cortical micro-stimulation (ICMS; 150 msec trains of .2 msec biphasic pulses at 300 Hz). The boundary between M1 and PMd was estimated on the basis of sulcal landmarks obtained during MRI scans and ICMS thresholds (thresholds for penetrations in M1 were $\leq$40 μA and those in PMd were $\leq$70 μA), and verified by histology (regions where the density of large pyramidal cells changed; Weinrich and Wise, 1982).

The signal from each electrode was amplified (10 K), band-pass filtered (300–6000 Hz), and fed to template matching devices to isolate the activity of up to three SUs per electrode (multi-spike detector (MSD), Alpha-Omega Engineering). Spikes and behavioral events were sampled at 1 kHz and logged on a custom data-acquisition system. During the tracing experiment only, the amplified extra-cellular signal was also band-pass filtered (1–10,000 Hz), sampled at 25 kHz (Alpha-Map 5.4, Alpha-Omega Engineering), and stored on disk for offline processing. Hand position was sampled at 100 Hz.

2.3. *Signal processing and neural database*

Offline, MUA was estimated by band-pass filtering the 25 kHz signal (300–6000 Hz, 3-pole Butterworth), clipping extreme values (larger or smaller than the mean ± 2 standard deviations [SDs]), and computing the sample-by-sample root-mean-square (raising to the 2nd power, low-pass filtering at 100 Hz, down-sampling to 500 Hz, and taking the square root; Stark and Abeles, 2007). The clipping was done to reduce the influence of high amplitude events, which presumably are mostly spikes of nearby neurons, but does not remove all their energy. To obtain MUA that does not depend at all on detectable spiking we computed a "de-spiked" MUA (dsMUA) as follows. First, we de-spiked the raw extra-cellular voltage by leaving only the noise above ~5000 Hz in the record. This was done by computing the difference between each spike and a "smoothed" spike obtained by convolving the spike with a 5-point rectangular kernel (spanning .2 msec; Fig. 2A). We then repeated MUA estimation, but from the de-spiked extra-cellular voltage (Fig. 2B); the amplitude of the resulting dsMUA was reduced around spike times and essentially unaltered elsewhere.

SU firing rate profiles were obtained by convolving spike trains with a Gaussian kernel (SD of 50 msec). MUAs were

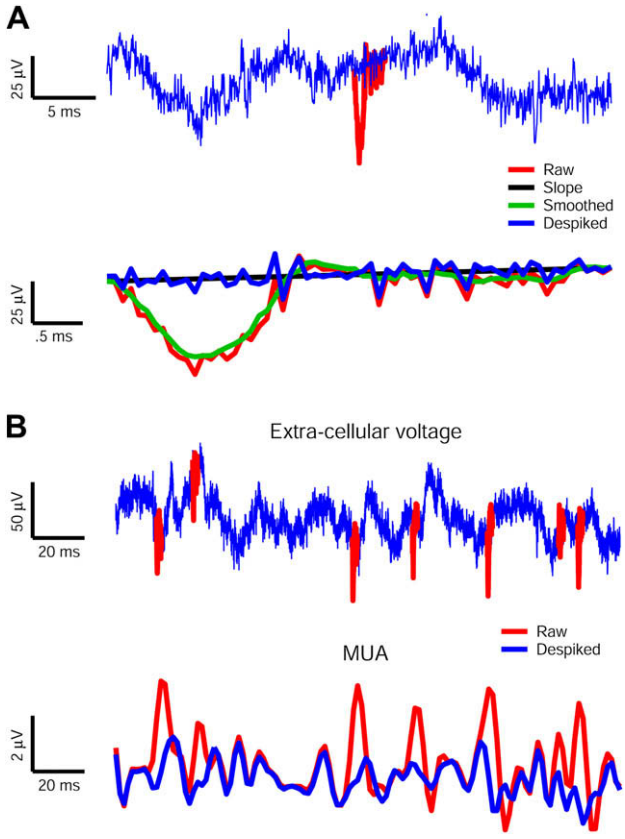

Fig. 2 – Illustration of "de-spiking" procedure. (A) Replacement of a single spike with high-frequency noise. *Top*: 40 msec record of raw neural activity (1000 samples at 25 kHz) with one spike (red). This spike is replaced with the blue trace as explained in the bottom panel. *Bottom*: expanded view of the spike (red) and the noise that replaced it (blue). The noise was obtained by computing the sample-by-sample difference between the original spike and a 5-point moving-average smoothed version of it (green) and adding this to a line (slope, black) connecting the first and last samples of the original spike. (B) Resulting MUA estimates. *Top*: 250 msec record of raw neural activity with several spikes; rightmost spike is from Fig. 2A. *Bottom*: MUA (red) and dsMUA (blue) estimated from the raw and de-spiked extra-cellular voltages, respectively. The dsMUA is considerably lower than the MUA when spikes have been removed and similar elsewhere.

processed in the same manner. Hand position was low-pass filtered (8 Hz) and velocity and acceleration were computed by taking the corresponding derivatives. Position and its time derivatives were expressed in units of cm and sec.

Individual channels (SUs and MUAs) considered for analyses were (1) well-isolated, as determined by spike waveforms and by inter-spike interval histograms (applicable only to SUs); (2) recorded during a subset of consecutive trials in which activity was first-order stationary. Stationarity was verified quantitatively by computing the mean activity in each trial and plotting it against the chronological trial number. Units that exhibited a significant linear trend (quantified by the correlation-coefficient and tested by trial shuffling; 1000 shuffles, $p < .05$; Paninski et al., 2004) were not considered; (3) the firing rate (of the SU; for MUA, of all spikes recorded by the electrode) was at least 1 spikes/sec; (4) the total duration of all considered movement periods was at least 2.5 min. For scribbling movements, the first 200 msec following a reward were excluded. For tracing movements, the considered movement periods started once the monkey began to follow the path and ended once the end of the path was arrived at, before reward was delivered.

Using the above criteria, a total of 277 SUs (105/172 during scribbling/tracing, respectively) and 124 MUAs (tracing only) were subjected to further analyses. SUs were recorded during 115/157 stationary trials (medians; 95% ranges, 63–290/54–296) for a total duration of 4.4/7.4 min (medians; 95% ranges, 2.6–10.4/2.8–14 min). MUAs provide a more stable signal than do SUs (Stark and Abeles, 2007), and to facilitate SU–MUA comparisons based on similar sample sizes we employed only the first 150 stationary trials of each record.

2.4. Data analysis

Neural activity (SU firing rate or MUA) was modeled as a linear function of movement

$$F(t) = c + \sum_{i=0}^{2} a_i f\left(x^{(i)}(t+\tau_i), y^{(i)}(t+\tau_i)\right). \quad (1)$$

In Eq. (1), the superscript (i) denotes the ith derivative of position with respect to time, and τ_i indicates that the ith derivative is lagged τ time samples relative to the neural activity. The value of τ can be positive or negative; positive values correspond to neural activity leading movement. Thus, the neural activity F at time t is a function of the position (x, y) at time $t+\tau_{pos}$, the velocity vector $\vec{v}$ at time $t+\tau_{vel}$, and the acceleration vector $\vec{a}$ at time $t+\tau_{acc}$. Individual components were modeled using cosine functions. Specifically for position, a cosine function was employed because the firing of many SUs appeared to be higher in specific parts of the workspace without an apparent monotonous gradient as implied by a planar model (Kettner et al., 1988; Paninski et al., 2004) and the cosine model was found to describe motor cortical activity well without resorting to non-linear modeling (e.g., Gaussian; Aflalo and Graziano, 2006). Note that the cosine model has two more free parameters than the planar model. The width of the cosine was chosen so as to allow for a single peak in the workspace; for derivation, additional details, and comparisons with other linear, auto-regressive, and non-linear models, see Stark et al. (2007b). Under these circumstances, Eq. (1) can be rewritten as

$$\begin{aligned} F(t) =& b_0 + b_1 \cos kx(t+\tau_{pos}) + b_2 \sin kx(t+\tau_{pos}) \\ &+ b_3 \cos ky(t+\tau_{pos}) + b_4 \sin ky(t+\tau_{pos}) \\ &+ b_5 \|\vec{v}(t+\tau_{vel})\| \\ &+ b_6 \|\vec{v}(t+\tau_{vel})\| \cos \theta_{vel}(t+\tau_{vel}) \\ &+ b_7 \|\vec{v}(t+\tau_{vel})\| \sin \theta_{vel}(t+\tau_{vel}) \\ &+ b_8 \|\vec{a}(t+\tau_{acc})\| \\ &+ b_9 \|\vec{a}(t+\tau_{acc})\| \cos \theta_{acc}(t+\tau_{acc}) \\ &+ b_{10} \|\vec{a}(t+\tau_{acc})\| \sin \theta_{acc}(t+\tau_{acc}), \end{aligned} \quad (2)$$

where k is a space constant determining the width of the position cosine (we used $k = 2\pi/10$ which, given workspace sizes, resulted in symmetric uni-modal surfaces), $\|\vec{v}\|$ is the magnitude of the velocity vector (speed), θ_{vel} is its direction, and time lags range from −300 to 300 msec at 10 msec resolution. For each given combination of lags (τ_{pos}, τ_{vel}, τ_{acc}) the coefficients b_i ($i = 1,\ldots,10$) in Eq. (2) and the total R^2 were estimated using multiple linear regression. The R^2 is the overall fraction of variance in neural activity associated with the movement parameters included in the analysis. In this study, the R^2 is therefore a function of three time lags, and can be visualized as a three-dimensional cube (Fig. 3C, bottom) in which each axis measures the time lag between neural activity and a different movement parameter: position (horizontal), velocity (vertical), and acceleration (depth), and each of the three faces shows the marginal mean R^2 at the corresponding dimension.

To measure the influence of each parameter on neural activity we employed a measure of contribution, estimated at multiple time lags:

$$C_i(\tau_{pos}, \tau_{vel}, \tau_{acc}) = \frac{b_i(\tau_{pos}, \tau_{vel}, \tau_{acc}) \cdot \sigma_i \cdot \rho_i(\tau_i)}{\sigma_F}, \quad (3)$$

where b_i is the regression coefficient corresponding to the ith parameter ($i = 1,\ldots,10$) at time lag combination (τ_{pos}, τ_{vel}, τ_{acc}), σ_i is the SD of that parameter, $\rho_i(\tau_i)$ is the pair-wise (Pearson) correlation-coefficient between neural activity F and parameter i at time lag τ_i, and σ_F is the SD of F (Stark et al., 2007b). For each combination of time lags the sum of all contributions equals the R^2. Thus, the contribution of a specific parameter can be interpreted as a fraction of the total R^2, namely the portion of movement-related firing rate variance associated with that parameter, taking into account all other parameters, at a given combination of time lags. The contributions of different parameters of the same time derivative (position, velocity, or acceleration) were combined, yielding C_{pos}, C_{vel}, C_{acc} (Fig. 3C, top three cubes).

Neural activity was considered to be movement-related if the maximal R^2 over all time lag combinations was significant at a level of .0001, determined using a permutation test (10,000 shuffles; Stark et al., 2007b). The unusually low alpha level was chosen to account for the multiple comparisons that stem from the many combinations of time lags, and corresponds to a conservative estimate of a corrected level lower than .01 (for a cube spanning 600^3 msec estimated for spike trains smoothed by a Gaussian kernel with SD of 50 msec there are less than 100 independent measurements).

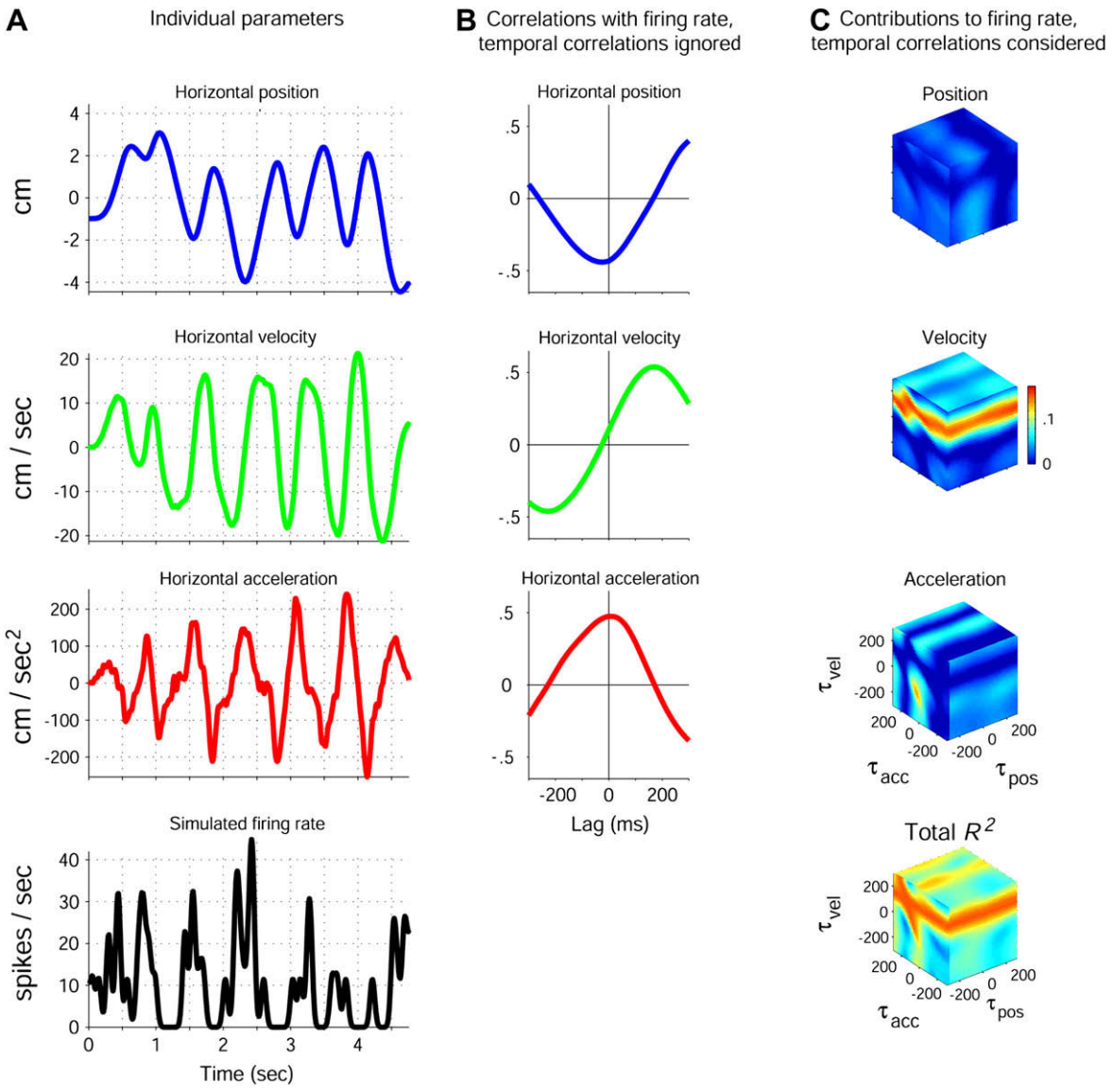

Fig. 3 – Illustration of temporal correlation analysis. (A) Movement parameters and simulated neural activity. *Top three panels* show horizontal components of position, velocity, and acceleration during a single tracing trial. Peaks in the position curve are typically preceded by velocity peaks by ~200 msec, and peaks in velocity by peaks in acceleration by another ~200 msec. Thus, while movement parameters are typically uncorrelated at zero-lag, delayed correlations are much higher. *Bottom panel* shows the simulated firing rate, during the same trial, of a putative neuron with a cosine relation to velocity direction: $F(t) = 10 + 6\cos\theta_{vel}(t + 150)$; θ_{vel} was derived from real movements. $F(t)$ is the noiseless firing rate at time t and $\theta_{vel}(t + 150)$ is the direction of the velocity vector 150 msec later. $F(t)$ was treated as a time-varying Poisson process and spikes were generated by deciding at every millisecond whether a spike was or was not fired. The artificial spike train was then processed exactly like spike trains recorded in experiments. (B) Correlations between movement parameters and neural activity are ambiguous. Neural activity was simulated strictly according to θ_{vel} but was, at zero-lag, negatively correlated with position (*top panel*) and positively correlated with acceleration (*bottom panel*). (C) Consideration of temporal correlations and use of contributions enables correct determination of the encoded parameter. *Top three panels* show, from top to bottom, the contribution of position (taking into account velocity and acceleration), velocity (taking into account position and acceleration), and acceleration (taking into account position and velocity) to the movement-related firing rate variance. In each cube, each axis measures the time lag between neural activity and a different movement parameter: position (horizontal), velocity (vertical), and acceleration (depth); axis labels are detailed at the bottom (acceleration) cube and indicated by small ticks in the two other cubes. Positive lags correspond to neural activity coming before movement. For each cube, each of the three faces shows the marginal mean contribution at the corresponding dimension; color scale is the same for all cubes. There are stripes of relatively high contribution on the velocity cube and not on any other cube. These stripes are at a time lag of 150 msec and indicate a contribution of movement velocity to the firing rate that preceded it by 150 msec. *Bottom panel* shows the overall fraction of firing rate variance associated with movement, the R^2, at each time lag combination; for each time lag combination, the R^2 is the sum of all contributions. In this simulation, the maximal R^2 is .16. The stripes with highest R^2 values on the velocity–acceleration face (left) and on the velocity-position face (right) at a time lag of 150 msec are consistent with the simulated parameter (velocity) and time lag (150 msec).

After determining that neural activity was movement-related, we determined which of the three parameters contributed to the neural activity variance and at what time lags. For artificial neural activity related to velocity, there is a plane of high values in the velocity cube, at a constant τ_{vel} for all τ_{pos}s and all τ_{acc}s (Fig. 3C). We therefore looked for parameters that were related to firing rate at a constant time lag, manifesting as a plane slicing through the relevant contribution cube. To this end, we operationally defined a dominant relation to a movement parameter at a given lag as a cube's plane at that lag in which at least half of the time lag combinations each contributes more than max(R^2)/2; if most time lag combinations are high and contiguous a plane is detected (for additional details, see Stark et al., 2007b). This definition allows detecting up to one plane in each orientation at the same time lag relative to the firing rate, allowing multiple parameters to be dominant at the same time lag relative to the neural activity (as in Fig. 4A, right).

Finally, we determined the values of encoded parameters. For PDs of movement velocity, this was the arctangent of ratio between the *y* and *x* standardized regression coefficients (beta weights), or

$$PD_{vel} = \tan^{-1}\left(b_{y^{(1)}}\sigma_{y^{(1)}}\right)\Big/\left(b_{x^{(1)}}\sigma_{x^{(1)}}\right), \quad (4)$$

resolved to the proper quadrant, where $x^{(1)}$ and $y^{(1)}$ are the horizontal and vertical velocities as defined in Eq. (1). A corresponding expression was used for acceleration PDs. Since many time lag combinations provided meaningless coefficients (i.e., with insignificant R^2s), PDs were evaluated only at the time lag of the corresponding parameter (e.g., for velocity PDs, at τ_{vel}) but averaged over all time lags of the other parameters (e.g., for velocity PDs, τ_{pos}s and τ_{acc}s) that contributed more than half of the maximal R^2 (for illustration, see Stark et al., 2006). An identical procedure was carried out for the horizontal and vertical coordinates of preferred positions.

3. Results

3.1. *Explicit consideration of temporal correlations between drawing parameters resolves ambiguities in neural encoding*

Two monkeys were trained to perform drawing movements (Fig. 1). One monkey was trained to make free scribbling movements (Fig. 1A) and another to trace given paths (Fig. 1B). Both tasks yielded a rich sampling of drawings (see Fig. 1, bottom, for some examples) and covered a wide range of movement speeds, directions, and accelerations. Moreover, zero-lag correlations between the three kinematic parameters examined here – position, velocity, and acceleration – were close to zero (scribbling, .01 ± .03, mean ± SD of 18 sessions; tracing, .015 ± .004, 22 sessions). However, temporal correlations between parameters persisted at non-zero lags: for instance, to scribble in the right side of the working plane, the arm first needs to move there. This is manifested as a peak in horizontal position preceded by a peak in velocity by about 200 msec (Fig. 3A, two top panels). Furthermore, peaks in velocity were typically preceded by peaks in acceleration (Fig. 3A, two central panels).

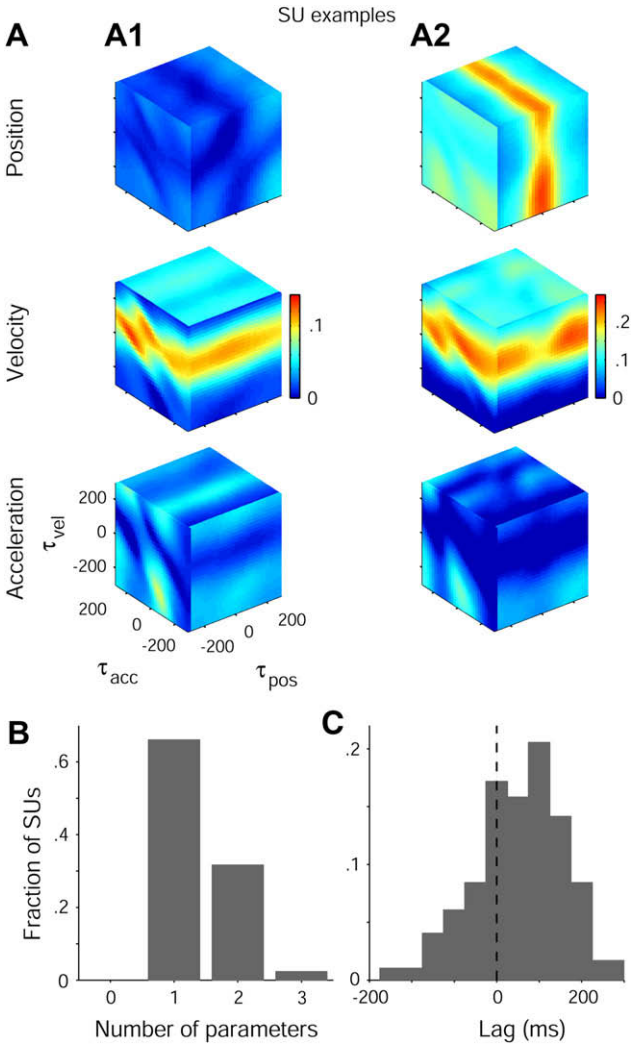

Fig. 4 – SU properties during drawing. (A) Examples of SUs related to drawing kinematics. *Left*: SU activity related to a single parameter, drawing velocity, peaking at a time lag of 70 msec irrespective of the delay with either position or acceleration. The maximal R^2 for this unit is .15. Conventions are the same as in Fig. 3C. *Right*: SU activity related to two parameters, position and velocity. Time lag is 0 msec for position and 90 msec for velocity. The maximal R^2 is .37. (B) Number of parameters represented by SUs. Two-thirds (144/218) of the movement-related units represent a single parameter. (C) Time lags of represented parameters. There are 297 represented parameters and bin width is 50 msec. Although time lags are widely dispersed, there is a tendency for lags to be positive, corresponding to neural activity coming before movement.

The strong temporal correlations between movement parameters result in potentially ambiguous interpretations of unambiguous neural activity. For purposes of illustration we simulated neural activity based on the direction of arm movement according to a simple cosine model, $F(t) = 10 + 6\cos\theta_{vel}(t + 150)$ (Fig. 3A, bottom). In this model, neural activity precedes movements directly to the right by

150 msec. Accordingly, the correlation between neural activity and horizontal velocity peaks at about 150 msec (Fig. 3B, center). However, due to the temporal correlations between movement parameters, neural activity is also strongly correlated with position and acceleration at zero-lag (Fig. 3B, top and bottom panels). Similar results are obtained when zero-lag correlations between parameters are taken into consideration in a multiple linear regression framework (not shown here; see Stark et al., 2006, 2007b).

In contrast, when *temporal* correlations between parameters are explicitly taken into account, it becomes clear that the neural activity is related predominantly to velocity (Fig. 3C, top three panels). Note that instead of correlation or regression coefficients, the contribution of each parameter to the overall firing rate variance is shown in these cubes (Eq. (3)). Thus, each cube shows the contribution of one parameter (e.g., velocity, at center) to the firing rate variance at all relevant time lags (here, −300 to 300 msec before the movement, with positive lags corresponding to neural activity coming before movement), taking into account the other parameters (e.g., position and acceleration) at all possible time lag combinations. In short, by explicitly considering temporal correlations and computing contributions instead of correlations, the neural activity was found to be related exclusively to velocity at a time lag of 150 msec, exactly as simulated.

3.2. *SU activity during drawing movements*

Analyzing SUs recorded from the motor cortices of monkeys during drawing we found that most SUs were related to one parameter and only a minority to more than one parameter; Fig. 4A shows two examples. Since these results have been reported in detail elsewhere (Stark et al., 2007b) they are only briefly summarized in this paragraph. Of 277 tested SUs, 218 were movement-related (resampling test, $p < .01$), and of these, most (144, 66%) were related to a single parameter (Fig. 4B). The excess of units related to exactly one parameter was significant (χ^2 goodness-of-fit test, 4×2 table, $N = 218$, $p \ll .001$). Since about a third of the units were related to more than one parameter, there were more "represented" parameters (297) than movement-related SUs (218). Although widely dispersed, SU activity tended to precede movement (one-tailed *t*-test, 297 represented parameters, $p \ll .001$), with a median time lag of 60 msec (Fig. 4C).

The most commonly represented parameter was velocity. Of the SUs related to a single parameter, 80% (115/144) were related to velocity; a similar result was obtained when all 297 represented parameters were considered (Fig. 5A). Parameter values were broadly sampled. Specifically, preferred positions spanned the entire working plane without clustering at any specific region (Fig. 5B). There was a lack of preferred positions at the workspace center, but statistical testing did not reveal significant deviations from uniformity (two Kolmogorov–Smirnov tests, comparing the horizontal and vertical distributions of preferred positions to uniform distributions, $N = 41$; $p = .9$ and $p = .15$, respectively; similar results were obtained when scribbling and tracing data were tested separately). PDs of movement velocity spanned the entire unit circle (Fig. 5C; Rayleigh test, $N = 187$; $p = .77$) and so did acceleration PDs (Fig. 5D; Rayleigh test, $N = 69$; $p = .93$).

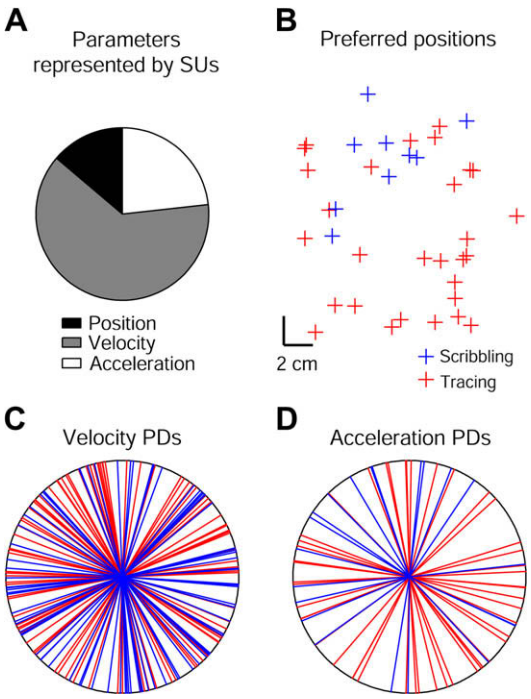

Fig. 5 – Parameters represented by SUs during drawing. (A) Identity of parameters represented by SUs. There are 218 movement-related SUs, and since some units represent more than one parameter (Fig. 4B) there are a total of 297 represented parameters. Velocity is most common. (B) Preferred positions of SUs representing position (41 SUs). Colors distinguish between scribbling (blue) and tracing (red) data. The preferred positions span the entire workspace. (C) PDs of SUs representing velocity (187 SUs). Velocity PDs distribute uniformly on the unit circle. (D) PDs of SUs representing acceleration (69 SUs). Acceleration PDs distribute uniformly on the unit circle.

To summarize, SUs recorded during drawing tended to prefer a single parameter, most often velocity, but position and acceleration were also represented. Over all units, preferred positions, velocity PDs, and acceleration PDs were widely distributed.

3.3. *Spatial organization of SU activity related to drawing parameters*

To test for spatial organization of SUs related to movement parameters, we first examined the identity of the encoded parameters as a function of inter-unit distance. For simplicity, the 218 movement-related SUs were paired in three ways, forming three sets: all possible pairs (218 choose 2 = 23,653 pairs), all pairs recorded from the same site (median inter-unit distance of approximately .8 mm, Stark and Abeles, 2007; 634 pairs), and all pairs recorded by the same electrode (median inter-unit distance of approximately 30 μm, Abeles, 1982; 57 pairs). We then determined a "preferred parameter" for each SU. For the 144 SUs related to one parameter, it was

simply that parameter, and for the other units it was the parameter that made the largest contribution to the movement-related firing rate variance. Over all 218 SUs, the preferred parameters were position, velocity, and acceleration in 30, 146, and 42 SUs, respectively. Thus the probability of a randomly-chosen pair of SUs to prefer the same parameter was .505 (sum of squared fractions of preferred parameters; see dashed line in Fig. 6A). Among SUs recorded from the same site, the observed probability to prefer the same parameter was slightly higher, .514, but among SUs recorded by the same electrode it was significantly higher, .614 (binomial test, $p = .034$).

Next, we tested for spatial organization of specific parameter values, namely preferred positions, velocity PDs, and acceleration PDs. The 41 position-related SUs formed a total of 820 pairs and 26 same-site pairs (but no same-electrode pairs). SUs recorded in the same site tended to have more similar preferred positions than SUs recorded in different sites (Fig. 6B), although this tendency was not significant (Mann–Whitney *U*-test, $p = .5$). The 187 velocity-related SUs formed a total of 17,391 pairs, 463 same-site pairs, and 44 same-electrode pairs. The expected difference between a randomly-chosen pair of velocity (or acceleration) directions sampled from a uniform distribution is 90° (dashed line in Fig. 6C). While pairs of randomly-chosen SUs had velocity PD-difference of $89 \pm .4°$ (mean ± SEM), SUs recorded from the same site had more similar PDs (PD-difference, $83 \pm 2.5°$), and SUs recorded by the same electrode had the most similar PDs (PD-difference, $64 \pm 8.1°$). Thus, the velocity PD-difference between pairs of SUs recorded by the same electrode was considerably smaller than the velocity PD-difference for randomly-chosen pairs of SUs (*U*-test, $p = .008$). Finally, similar results were obtained for acceleration PDs. The 69 acceleration-related SUs formed a total of 2346 pairs, 80

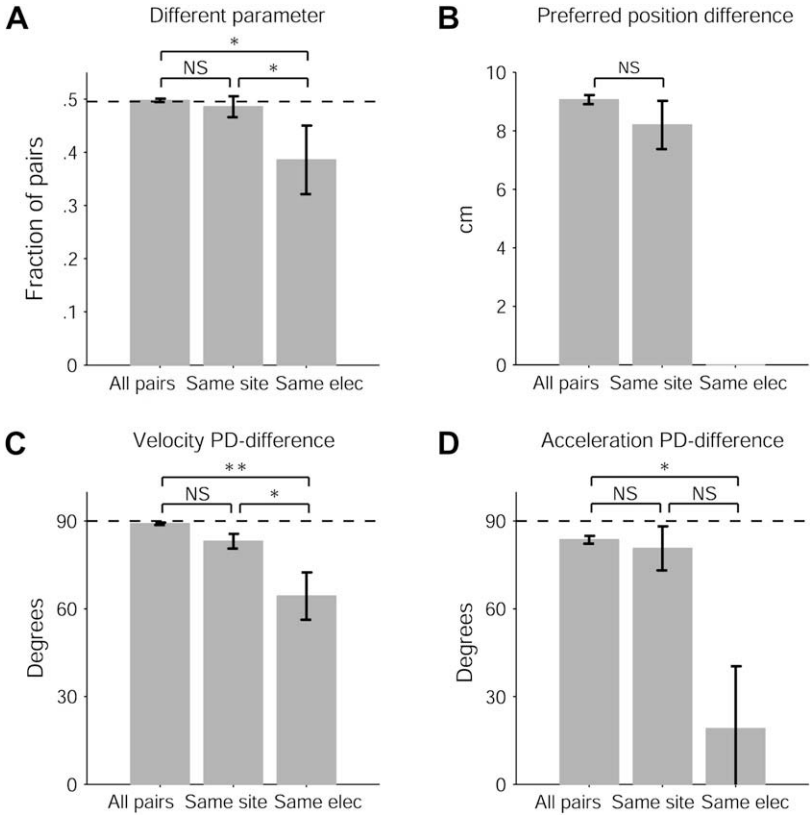

Fig. 6 – Spatial organization of parameters represented by SUs during drawing. (A) Difference between encoded parameters versus inter-unit distance. The 218 movement-related SUs were paired in three ways, forming three sets: all possible pairs (23,653 pairs), all pairs recorded from the same site (634 pairs), and all pairs recorded by the same electrode (57 pairs). Dashed line shows theoretical chance level (complement of the sum of squared fractions of preferred parameters) and stars indicate a significant difference between sets at the .05 level (binomial test); NS, not significant. Pairs of SUs recorded by the same electrode have the lowest probability to represent different parameters. (B) Difference between preferred positions versus inter-unit distance. The 41 position-related SUs formed a total of 820 pairs and 26 same-site pairs. SUs recorded in the same site tend to have more similar preferred positions than SUs recorded in different sites. (C) Difference between velocity PDs versus inter-unit distance. The 187 velocity-related SUs formed a total of 17,391 pairs, 463 same-site pairs, and 44 same-electrode pairs. Here and in Fig. 6D dashed line shows theoretical chance level (assuming random sampling from a uniform distribution of PDs) and single/double stars indicate a significant difference between sets at the .05/.01 level (Mann–Whitney *U*-test). Velocity PDs of SUs recorded by the same electrode are most similar. (D) Difference between acceleration PDs versus inter-unit distance. The 69 acceleration-related SUs formed a total of 2346 pairs, 80 same-site pairs, and six same-electrode pairs. Acceleration PDs of SUs recorded by the same electrode are most similar.

same-site pairs, and six same-electrode pairs. While acceleration PD-differences among randomly-chosen SUs were $84 \pm 1.3^\circ$ (mean ± SEM), the acceleration PD-differences among SUs recoded by the same electrode were $19 \pm 21^\circ$ (Fig. 6D; *U*-test, $p = .038$).

In sum, SUs recorded from the same site, and particularly by the same electrode, showed a weak but significant tendency to prefer the same parameter. Although parameter values of randomly-chosen SUs were uniformly distributed, SUs preferring the same parameter and recorded from the same site – and especially by the same electrode – tended to prefer somewhat similar values of that parameter. Thus, there was a tendency for nearby neurons to share similar encoding properties.

3.4. *MUA related to drawing kinematics*

The observation that pairs of SUs recorded in close proximity share similar properties suggests that activity in a local cluster of neurons might not "cancel out" completely but rather retain some information. Although properties of such local activity may be estimated by considering all spikes of all SUs recorded by an electrode, there are clearly other nearby neurons that cannot be detected in a given recording. Thus, instead of pooling together all discriminated spikes, we use another measure, MUA. The MUA is computed without discriminating spikes or isolating SUs but provides an estimate of the spiking activity of many neurons up to about 100–200 μm from the recording electrode (Legatt et al., 1980; Stark and Abeles, 2007).

Even assuming that nearby SUs have somewhat similar properties as shown in Section 3.3, it cannot be predicted whether the information in mass activity (MUA) would be higher or lower than in SUs. To address this issue we analyzed MUAs recorded during the tracing task (Fig. 1B) in the same manner SUs were analyzed; Fig. 7A shows a few examples. In each example, there is a clear relation between MUA and one movement parameter, as in the SU example shown in Fig. 4A (left). Moreover, the time lags are positive in all three examples, indicating that the illustrated MUAs tended to be active before movement. Finally, the R^2s in these examples are $\geq .2$, suggesting a robust relation to the represented movement parameter.[1]

When analyzing all 124 available MUAs in this manner, several properties became evident. First, MUAs were clearly related to tracing kinematics, just like SUs. Virtually all MUAs were movement-related (121/124, 98%; resampling test, $p < .01$). Consistent with this, the fraction of movement-related variance among MUAs was .2 (median R^2 of 124 MUAs), more than twice the corresponding fraction among all SUs recorded by the same electrodes (Fig. 7B; median R^2 of 172 SUs, .09; *U*-test, $p \ll .001$). Note that this statement is correct only on average, as there were some (rare) SUs with very high R^2s, as high as .78. Second, like SUs, MUAs were typically related to a single dominant movement parameter (Fig. 7C). Of the movement-related MUAs, most (65%, 78/121) were related to a single parameter (χ^2 goodness-of-fit test, 4×2 table, $N = 121$, $p \ll .001$). The distributions of the number of parameters represented by SUs and MUAs were similar to each other (χ^2 test of independence, 3×2 table, $p = .88$). Third, MUAs tended to be active before movement (Fig. 7D), with a median time lag of 60 msec (one-tailed *t*-test, 170 represented parameters, $p \ll .001$). This lag was not significantly different from the median time lag of parameters represented by SUs recorded by the same electrodes (50 msec; $N = 181$; *U*-test, $p = .47$). Fourth, although the most common parameter represented by both SUs and MUAs was velocity (of MUAs related to a single parameter, 47/78, 60%, were related to velocity, and a similar result was obtained for all 170 represented parameters, Fig. 7E), MUAs tended to be related to position more than SUs (χ^2 test of independence, 3×2 table, $p = .02$).

Thus, in addition to being related to drawing kinematics, MUAs shared the same properties as SUs regarding the number of represented parameters (typically one), the identity of the represented parameter (typically velocity), and the time lag to movement (typically positive). However, MUAs tended to have higher R^2s than SUs, yielding a more robust local signal.

3.5. *Relations between SUs and MUAs recorded by the same electrode*

Fig. 8A shows an example of two SUs and an MUA recorded simultaneously by the same electrode. All three channels were related to the same parameter, velocity, at a positive time lag. Moreover, the value of the encoded parameter was similar for the SUs and the MUA, as the velocity PDs of all three channels pointed towards the monkey (Fig. 8A, right). We also computed an dsMUA after removal of identified spikes, reflecting the activity of neurons further away from the recording electrode (Fig. 2), for which similar properties were obtained (see green arrow in Fig. 8A, right).

We examined whether SUs and dsMUAs recorded by the same electrode tended to be related to the same preferred parameter. There were 95 electrodes from which movement-related SUs and dsMUAs were recorded; these yielded a total of $95^2 = 9025$ pairs, 571 same-site pairs, and 95 same-electrode pairs. While the probability of randomly-chosen SU–dsMUA pairs to prefer the same parameter was .389 and that for same-site pairs was .392, the corresponding probability among same-electrode pairs tended to be higher, .463 (Fig. 8B; binomial test comparing all and same-electrode pairs, $p = .057$). We then tested the correspondence between the values of parameters encoded by SUs and dsMUAs. There were 67 electrodes from which a velocity-related dsMUA and at least one velocity-related SU were recorded. For each such

[1] Although these R^2 values might seem low, this is not the case. Some studies report R^2s on the order of .7 or even use this figure as a threshold for inclusion of units in analyses (for instance, Georgopoulos et al., 1982). However, such studies typically minimize variability in all except the tested parameter (using, for instance, center-out movements) and average data over time and trials. To illustrate this, we considered a model of cosine tuning to velocity direction and generated artificial firing rates on a sample-by-sample basis (as in Fig. 3A, bottom), employing movement data from center-out experiments (five trials per direction). Averaging firing rates across movement time and all trials from the same direction yielded a "tuning curve" for which the R^2s was typically high (median of 1000 runs: .93; 95% range: .75–.99). However, the R^2s estimated for exactly the same data but on a sample-to-sample and trial-to-trial basis were considerably lower, with a median of .17 (95% range: .09–.26). For more details see Stark et al. (2007b).

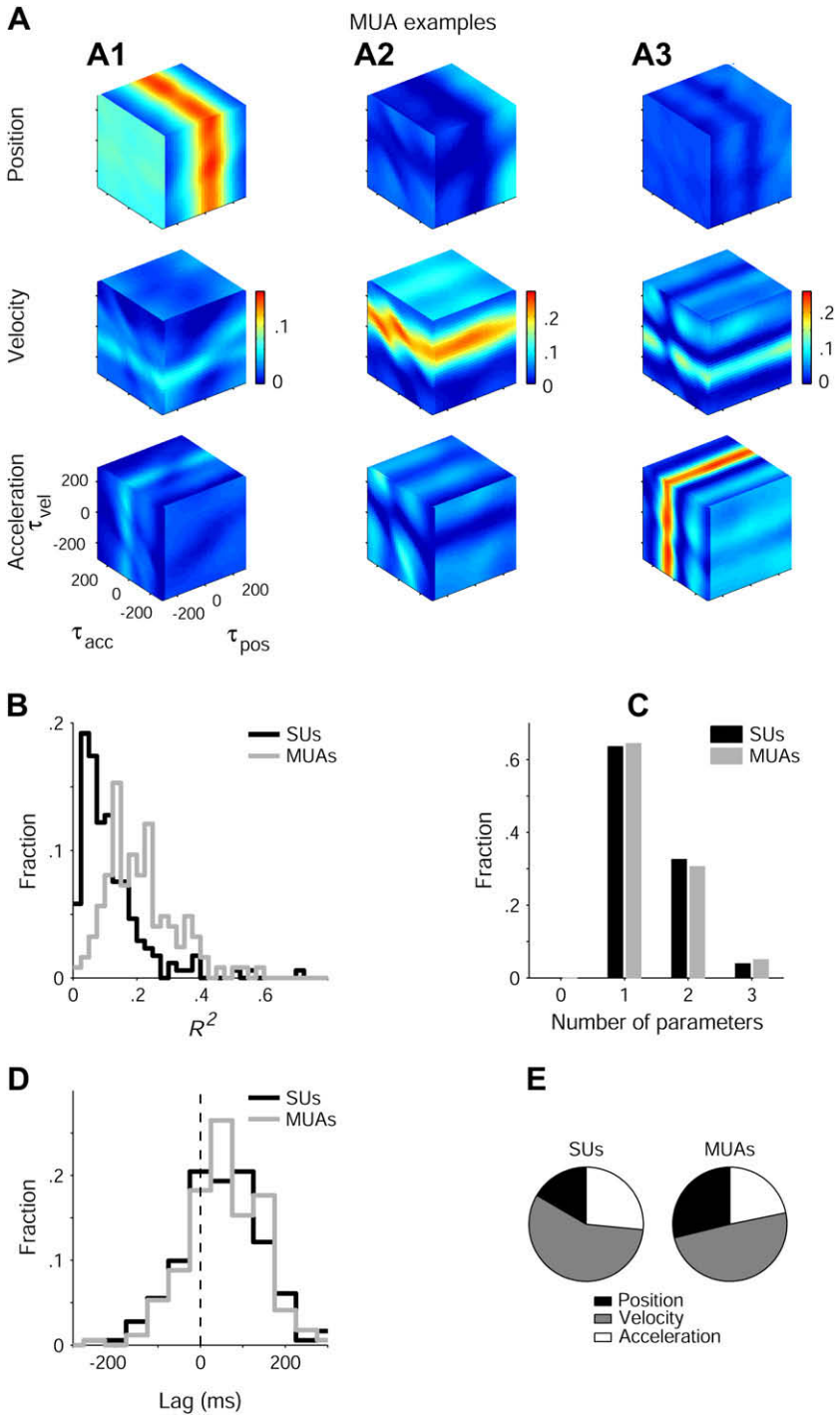

Fig. 7 – Properties of MUA during tracing. (A) Examples of MUAs related to tracing kinematics. *Left*: MUA related mainly to position. Time lag is 30 msec and maximal R^2 is .22. Conventions are the same as in Fig. 3C. *Center*: MUA related mainly to velocity. Time lag is 90 msec and R^2 is .26. *Right*: MUA related mainly to acceleration. Time lag is 60 msec and R^2 is .32. (B) Distribution of R^2 of SUs and MUAs during tracing. For each SU and MUA, the maximal R^2 over all time lag combinations was noted. Histogram contains all SUs (172) and MUAs (124) recorded during tracing; bin width is .025. MUAs have higher R^2 than SUs. (C) Number of parameters represented by SUs and MUAs. Samples include all movement-related SUs (129) and MUAs (121) recorded during tracing. Other conventions are the same as in Fig. 4B. Both SUs and MUAs tend to be related to a single parameter. (D) Time lags of parameters represented by SUs and MUAs. Samples are the same as in Fig. 7C and conventions are the same as in Fig. 4C. Time lags of both SUs and MUAs tend to be positive. (E) Identity of parameters represented by SUs and MUAs. There are 181 and 170 parameters represented by SUs and MUAs, respectively. Position is more commonly represented by MUAs than by SUs, but velocity is most common among both signal types.

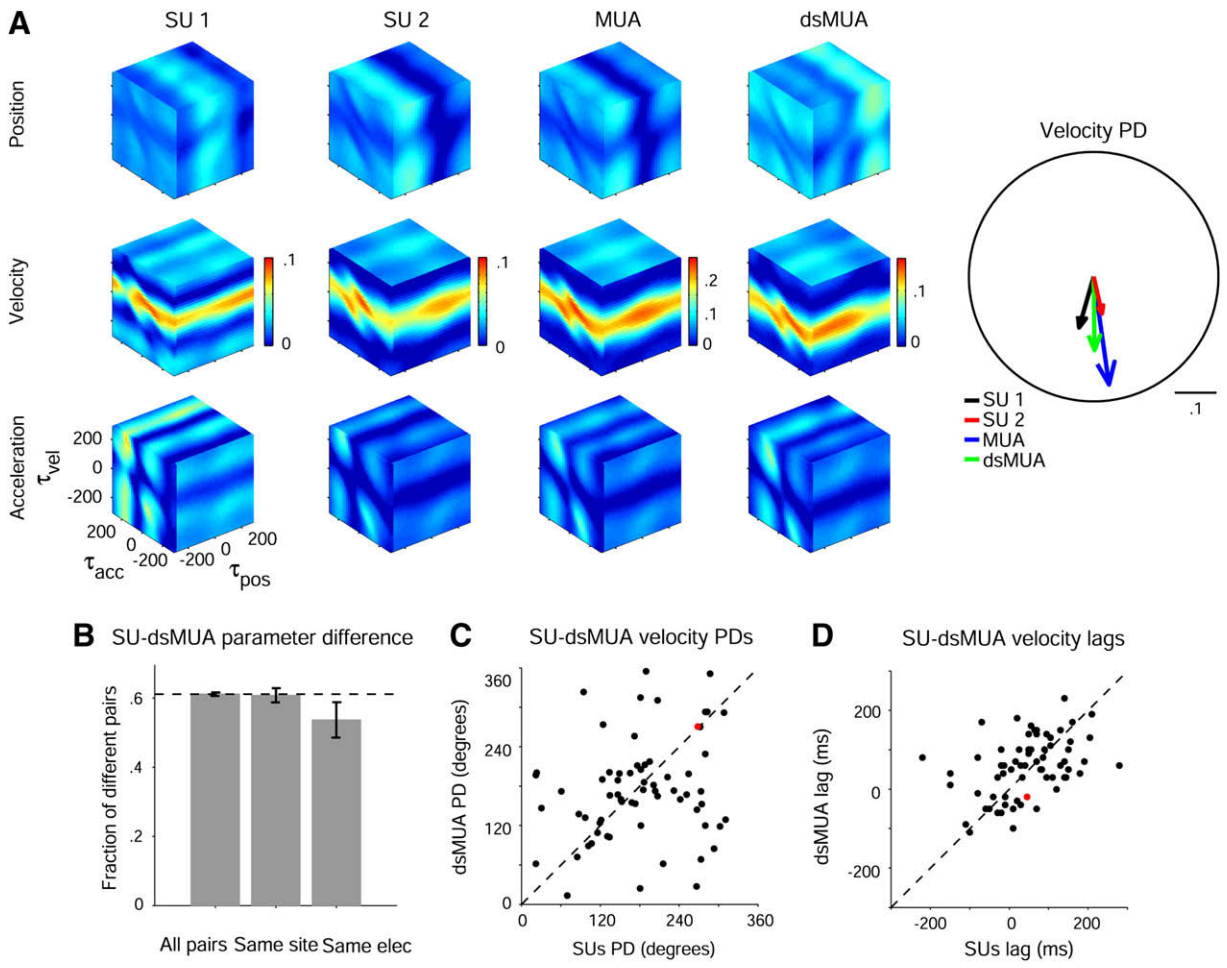

Fig. 8 – Correspondence between properties of SUs and MUA during tracing. (A) Example of two SUs and an MUA recorded by the same electrode. All three channels are related mainly to velocity, as was the de-spiked MUA (dsMUA). The polar plot (*right*) summarizes coding properties by vectors whose lengths correspond to each channel's R^2 and whose directions correspond to the PDs. The four vectors point in approximately the same direction. (B) Dependence of difference between parameters encoded by SUs and dsMUAs on anatomy. There were 95 electrodes from which both movement-related SUs and movement-related dsMUAs were recorded. These formed a total of 9025 pairs, 571 same-site pairs, and 95 same-electrode pairs. Conventions are the same as in Fig. 6A. SUs and dsMUAs recorded by the same electrode tend to be related to the same parameter. (C) Correspondence between velocity PDs of SUs and dsMUAs recorded by the same electrode. There were 67 electrodes from which velocity-related SUs and dsMUAs were recorded. For these, the velocity PDs are similar. The red dot corresponds to the example shown in Fig. 8A. (D) Correspondence between velocity time lags of SUs and dsMUAs. Sample size and conventions are the same as in Fig. 8C. Time lags of SUs and dsMUAs recorded by the same electrode are similar.

electrode we noted the velocity PDs of the dsMUA and the SUs; if more than one velocity-related SU was recorded by a given electrode (as in Fig. 8A), their PDs were averaged. As shown in Fig. 8C, the PDs of SUs and dsMUAs recorded by the same electrode were positively correlated (correlation-coefficient, .22; *t*-test, $p = .04$). A similar result was observed between the velocity PDs of the same SUs and raw MUAs (correlation-coefficient, .52; *t*-test, $p \ll .001$). Also, similar results were obtained for position- and acceleration-related SUs and dsMUAs recorded by the same electrode (data not shown). Finally, the time lags of SUs and dsMUAs were also positively correlated (Fig. 8D; correlation-coefficient, .42; $N = 67$; *t*-test, $p < .001$). In short, SUs and dsMUAs recorded by the same electrode tended to encode similar values of the same parameter at a similar time lag.

4. Discussion

We saw that during drawing, a single neuron is typically related to a single kinematic parameter, most often velocity, and that neurons at close proximity tend to share similar properties. Consistent with this, the MUA, which is an estimate of spiking activity around a recording electrode, is movement-related. In fact, MUAs are more robustly modulated by drawing kinematics than SUs. In all other aspects, MUAs

closely resemble SUs. Finally, dsMUAs and SUs recorded from the same electrode display similar properties, tending to encode similar values of the same parameter at similar time lags.

4.1. *Spatial organization in motor cortex*

Over the past century there have been multiple attempts to generate spatial maps of muscles and body parts in motor cortex (somatotopical organization; for a review, see Schieber, 2001). The spatial organization of more abstract movement parameters on the cortical surface has been studied much less. Using data from center-out tasks it was shown that nearby neurons tend to have similar PDs (Amirikian and Georgopoulos, 2003; Ben-Shaul et al., 2003). This property was later shown to be specific to neurons recorded from arm-related, but not finger-related, sites (Stark et al., 2007a). However, the methods used to collect and analyze these data were insufficient to determine the common parameter since multiple kinematic parameters were correlated in these tasks.

The current study demonstrated the existence of local spatial organization of motor cortical activity using two approaches. First, we directly measured the similarity between single neuron properties after taking into consideration temporal correlations between parameters. This extended the previous studies in three ways: the identity of the preferred parameter (position, velocity, or acceleration), its value (preferred positions, velocity PDs, and acceleration PDs), and its time lag. Second, we used indirect measurements of the activity of many neurons (MUA), and showed that MUAs retain information about movement despite the massive spatial averaging that takes place during their estimation.

The spatial range of activity captured by the MUA estimated from a single electrode is on the order of 100–200 μm (Legatt et al., 1980; Stark and Abeles, 2007). This range roughly corresponds to anatomical estimates of pyramidal cell aggregates which are 300 μm wide in the motor cortex (Meyer, 1987) and to the suggested width of functional cortical columns (Mountcastle, 1978). Thus, the current results might seem to support a modular organization of motor cortex. However, differences between neighboring SUs (recorded by the same electrode) were often considerable, inconsistent with a strict modular organization of motor cortex.

In contrast to a prior notion (Ashe and Georgopoulos, 1994; Fu et al., 1995; Paninski et al., 2004), we recently reported that during drawing, a motor cortical neuron is typically related to one kinematic parameter (Stark et al., 2007b). As discussed therein, we attribute the novelty of this finding to two key properties of our work. First, the movement space was sampled broadly, enabling a wider representation of all combinations of position, velocity, and acceleration than in previous work. Second, we explicitly considered temporal correlations between the tested parameters, and, while previous studies forced a fixed delay between firing rate and all movement parameters, we allowed each one to have its own specific delay. However, even if each neuron is related to one parameter during a given task, it remains to be explained how the MUA, and in particular the dsMUA, is also typically related to one dominant kinematic parameter. A-priori, there are at least two possibilities. One is that some neurons are more dominant than others (e.g., have higher firing rates) and therefore the MUA properties are similar to the properties of these neurons. If this was the case, uni-parametric relations would be expected to be less frequent among dsMUAs, contrary to what was observed. Also, SUs with properties similar to the MUA properties would be expected to have higher firing rates than SUs with dissimilar properties, which was not observed either (correlation-coefficient between SU firing rate and SU-MUA velocity PD-difference, −.03; $N = 99$; t-test, $p = .4$). Thus, it is unlikely that MUA is uni-parametric due to selective influence of specific neurons.

A second possibility is that during spatial averaging (MUA estimation) neurons with similar properties (e.g., related to similar values of the same parameter) make an accumulated contribution, while neurons with dissimilar properties (e.g., related to different parameters or opposite PDs) do not. This possibility is consistent with the tendency of nearby neurons to represent similar values of the same single parameter. Moreover, the observation that neurons further away from an electrode (quantified by the dsMUA in Fig. 8) are related to similar values of the same parameter as neurons closer to it (quantified by SUs) suggests that accumulation is not limited to the nearby neurons. Thus, it seems that similar processes influence motor cortical neurons closer and further away from the recording electrode.

A recent study found evidence for some periodic spatial structure of PDs in the motor cortex (Georgopoulos et al., 2007). However, we did not find any evidence for orderly maps of drawing parameters on the cortical surface in the current data as found in primary visual cortex; nor did others (Naselaris et al., 2006). Thus, movement parameters appear to be spatially organized only on a local scale. If, however, cortical maps of movement parameters do exist, the relations between them and the typically patchy somatotopical maps of muscles and/or body parts (Schieber, 2001) await future studies. In visual cortex, maps of several uncorrelated parameters appear to coexist (Hubener et al., 1997). In a single site in motor cortex, neurons related to one property (e.g., reach direction) coexist with neurons related to another property (grasp type), and independently of whether the site is arm- or finger-related (Stark et al., 2007a). Thus although orderly maps of kinematic parameters do not appear to exist in the motor cortex, neural activity in a given local region may still be related to several uncorrelated parameters (Stark and Abeles, 2007).

4.2. *Methodological considerations and interpretational limitations*

Previous studies of motor cortical activity in relation to movement typically used single-joint flexion/extension (Evarts, 1968) or center-out tasks (Georgopoulos et al., 1982). In these tasks, even under loading conditions (Thach, 1978), it is difficult if not impossible to distinguish between several kinematic parameters. In the current drawing tasks, correlations between parameters were negligible at zero-lag, and even the maximal temporal correlations were less than unity, enabling separation of the examined kinematic parameters.

By explicitly considering temporal correlations between the tested parameters, we were able to differentiate between movement parameters and estimate their time lags and values (preferred positions and directions).

The behavioral data used in this study were drawing movements. While considerably more broad than movement data used in most previous studies of motor cortical activity, drawings are typically confined to a small planar region and carried out under approximately fixed loading conditions and therefore comprise only a subset of the full range of natural movements. Although the current results were consistent between the two drawing tasks, whether other datasets are consistent with these results is an issue for future work. It is important to note, however, that any study seeking to correlate neural activity with movement parameters should broadly sample the relevant movement space (as done here for 2D drawings, and elsewhere for 3D movements; Aflalo and Graziano, 2006; Jackson et al., 2006) and explicitly consider temporal correlations between the tested parameters.

Since there is practically an infinite number of movement parameters and coordinate frames (kinematic, kinetic, intrinsic, extrinsic, Euclidean, non-Euclidean, and so on) that may be tested in relation to neural activity, the point of this work was not to test all of them. Rather, we focused on three kinematic parameters that together fully characterize drawing trajectories (position in time) regardless of muscle dynamics. Within these boundaries, we found that single neurons and MUAs are typically related to a single parameter and that nearby neurons share similar properties.

4.3. *Neural activity related to kinematic parameters*

Focusing on movement kinematics, we found that while most SUs and MUAs were related mainly to velocity, others were related mainly to the instantaneous position of the hand: this is in keeping with previous studies (Ashe and Georgopoulos, 1994; Paninski et al., 2004). Yet the fraction of MUAs that were predominantly related to position was higher than the corresponding fraction of SUs (29% *vs* 17%; Fig. 7E), suggesting that local spatial organization of position is more robust than of velocity. However, the effect was rather weak, necessitating more work to investigate this issue.

About a fourth of the SUs (and the MUAs) were predominantly related to acceleration. Previous studies of movement kinematics during straight reaching movements have found this fraction to be negligible (Ashe and Georgopoulos, 1994), presumably because the directions of the velocity and acceleration vectors are co-linear in such tasks (Stark et al., 2006).

4.4. *Functional implications*

The tendency of single neurons to be related to a single kinematic parameter suggests that distinct neurons partake in local networks related to distinct movement parameters. The similarities between nearby neurons and the tendency of MUAs to be related to a single kinematic parameter suggest that there is some anatomical ordering of these putative networks. However, the correspondence between neurons recorded within a small region (whose activity is captured by one MUA) was not perfect, and within it there were also neurons with other properties. This was shown here for the drawing tasks and elsewhere for prehension movements (Stark et al., 2007a). Thus, there is no perfect segregation of motor cortical neurons into well-defined specialized columns, but rather a local aggregation of neurons with similar properties, interleaved with other neurons that have dissimilar properties. This loose structure, combined with horizontal connections reported to link motor cortical sites millimeters apart (Huntley and Jones, 1991; Dum and Strick, 2005), may provide a basis for the coordination between distinct movement parameters (for instance, reach and grasp; position and direction) that is necessary for generating complex movements.

The observation that, on average, MUAs encode movement parameters more robustly than SUs is consistent with a recent decoding study showing that the combined activity of multiple MUAs provides more accurate predictions of movement than do multiple SUs (or multiple local field potentials; Stark and Abeles, 2007). Together, these findings demonstrate that it is possible for neurons in the brain to receive specific information from a given region without the need to be selectively connected to specific types of neurons within that region. Recently, it has been demonstrated that the activity of single neurons can be used to aid the paralyzed (Hochberg et al., 2006). Taken together, our findings demonstrate that MUAs provide a more robust control signal than SUs during both prehension and drawing movements and may be better suited for readout purposes by motor cortical prosthetic devices. We therefore expect that MUA-based, or MUA-enhanced, prosthetic devices, will perform more accurately and maintain their accuracy for a longer duration than SU-based devices. Clearly, real-time neuro-engineering work is required to validate this expectation.

Acknowledgements

We thank Itay Asher, Yoram Ben-Shaul, Gadi Goelman, Zoltan Nadasdy, Moshe Nakar, and Varda Sharkansky for help. We are grateful to Alit Stark for critical comments and discussions. This study was supported in part by a Center of Excellence grant (1564/04) administered by the Israel Science Foundation and the Deutsch-Israelische Projectkooperation.

REFERENCES

Abeles M. *Local Cortical Circuits*. Berlin: Springer-Verlag, 1982.

Aflalo TN and Graziano MS. Partial tuning of motor cortex neurons to final posture in a free-moving paradigm. *Proceedings of the National Academy of Sciences of the United States of America*, 103: 2909–2914, 2006.

Amirikian B and Georgopoulos AP. Modular organization of directionally tuned cells in the motor cortex: is there a short-range order? *Proceedings of the National Academy of Sciences of the United States of America*, 100: 12474–12479, 2003.

Ashe J and Georgopoulos AP. Movement parameters and neural activity in motor cortex and area 5. *Cerebral Cortex*, 6: 590–600, 1994.

Ben-Shaul Y, Stark E, Asher I, Drori M, Nadasdy Z, and Abeles M. Dynamical organization of directional tuning in the primate premotor and primary motor cortex. *Journal of Neurophysiology*, 89: 1136–1142, 2003.

Dum RP and Strick PL. Frontal lobe inputs to the digit representations of the motor areas on the lateral surface of the hemisphere. *Journal of Neuroscience*, 25: 1375–1386, 2005.

Evarts EV. Relation of pyramidal tract activity to force exerted during voluntary movement. *Journal of Neurophysiology*, 31: 14–27, 1968.

Fetz EE. Are movement parameters recognizably coded in activity of single neurons? *Behavioral and Brain Sciences*, 15: 679–690, 1992.

Fetz EE and Cheney PD. Postspike facilitation of forelimb muscle activity by primate corticomotoneuronal cells. *Journal of Neurophysiology*, 44: 751–772, 1980.

Flament D and Hore J. Relations of motor cortex neural discharge to kinematics of passive and active elbow movements in the monkey. *Journal of Neurophysiology*, 60: 1268–1284, 1988.

Fu QG, Flament D, Coltz JD, and Ebner TJ. Temporal encoding of movement kinematics in the discharge of primate primary motor and premotor neurons. *Journal of Neurophysiology*, 73: 836–854, 1995.

Georgopoulos AP, Kalaska JF, Caminiti R, and Massey JT. On the relations between the direction of two-dimensional arm movements and cell discharge in primate motor cortex. *Journal of Neuroscience*, 2: 1527–1537, 1982.

Georgopoulos AP, Merchant H, Naselaris T, and Amirikian B. Mapping of the preferred direction in the motor cortex. *Proceedings of the National Academy of Sciences of the United States of America*, 104: 11068–11072, 2007.

Hatsopoulos N, Joshi J, and O-Leary JG. Decoding continuous and discrete motor behaviors using motor and premotor cortical ensembles. *Journal of Neurophysiology*, 92: 1165–1174, 2004.

Hochberg LR, Serruya MD, Friehs GM, Mukand JA, Saleh M, Caplan AH, et al. Neuronal ensemble control of prosthetic devices by a human with tetraplegia. *Nature*, 442: 164–171, 2006.

Hubel D and Wiesel T. Receptive fields, binocular interaction and functional architecture in the cat's visual cortex. *Journal of Physiology (London)*, 160: 106–154, 1962.

Hubener M, Shoham D, Grinvald A, and Bonhoeffer T. Spatial relationships among three columnar systems in cat area 17. *Journal of Neuroscience*, 17: 9270–9284, 1997.

Humphrey DR, Schmidt EM, and Thompson WD. Predicting measures of motor performance from multiple cortical spike trains. *Science*, 170: 758–762, 1970.

Huntley GW and Jones EG. Relationship of intrinsic connections to forelimb movement representations in monkey motor cortex: a correlative anatomic and physiological study. *Journal of Neurophysiology*, 66: 390–413, 1991.

Imig TJ and Adrian HO. Binaural columns in the primary field (A1) of cat auditory cortex. *Brain Research*, 138: 241–257, 1977.

Jackson A, Mavoori J, and Fetz EE. Long-term motor cortex plasticity induced by an electronic neural implant. *Nature*, 444: 56–60, 2006.

Kettner RE, Schwartz AB, and Georgopoulos AP. Primate motor cortex and free arm movements to visual targets in three-dimensional space. III. Positional gradients and population coding of movement direction from various movement origins. *Journal of Neuroscience*, 8: 2938–2947, 1988.

Legatt AD, Arezzo J, and Vaughan Jr HG. Averaged multiple unit activity as an estimate of phasic changes in local neuronal activity: effects of volume-conducted potentials. *Journal of Neuroscience Methods*, 2: 203–217, 1980.

Meyer G. Forms and spatial arrangement of neurons in the primary motor cortex of man. *Journal of Comparative Neurology*, 262: 402–428, 1987.

Moran DW and Schwartz AB. Motor cortical representation of speed and direction during reaching. *Journal of Neurophysiology*, 82: 2676–2692, 1999.

Mountcastle VB. Modality and topographic properties of single neurons of cat's somatic sensory cortex. *Journal of Neurophysiology*, 20: 408–434, 1957.

Mountcastle VB. An organizing principle for cerebral function: The unit module and the distributed system. In Edelman GM, and Mountcastle VB (Eds), *The Mindful Brain*. Cambridge: MIT Press, 1978: 7–50.

Naselaris T, Merchant H, Amirikian B, and Georgopoulos AP. Large-scale organization of preferred directions in the motor cortex. II. Analysis of local distributions. *Journal of Neurophysiology*, 96: 3237–3247, 2006.

Paninski L, Fellows MR, Hatsopoulos NG, and Donoghue JP. Spatiotemporal tuning of motor cortical neurons for hand position and velocity. *Journal of Neurophysiology*, 91: 515–532, 2004.

Reina GA, Moran DW, and Schwartz AB. On the relationship between joint angular velocity and motor cortical discharge during reaching. *Journal of Neurophysiology*, 85: 2576–2589, 2001.

Riehle A and Requin J. Neuronal correlates of the specification of movement direction and force in four cortical areas of the monkey. *Behavioral Brain Research*, 70: 1–13, 1995.

Schieber MH. Constraints on somatotopic organization in the primary motor cortex. *Journal of Neurophysiology*, 86: 2125–2143, 2001.

Schwartz AB. Direct cortical representation of drawing. *Science*, 265: 540–542, 1994.

Schwartz AB, Moran DW, and Reina GA. Differential representation of perception and action in the frontal cortex. *Science*, 303: 380–383, 2004.

Stark E and Abeles M. Predicting movement from multiunit activity. *Journal of Neuroscience*, 27: 8387–8394, 2007.

Stark E, Asher I, and Abeles M. Encoding of reach and grasp by single neurons in premotor cortex is independent of recording site. *Journal of Neurophysiology*, 97: 3351–3364, 2007a.

Stark E, Drori R, and Abeles M. Partial cross-correlation analysis resolves ambiguity in the encoding of multiple movement features. *Journal of Neurophysiology*, 95: 1966–1975, 2006.

Stark E, Drori R, Asher I, Ben-Shaul Y, and Abeles M. Distinct movement parameters are represented by different neurons in the motor cortex. *European Journal of Neuroscience*, 26: 1055–1066, 2007b.

Thach WT. Correlation of neural discharge with pattern and force of muscular activity, joint position, and direction of intended next movement in motor cortex and cerebellum. *Journal of Neurophysiology*, 41: 654–676, 1978.

Todorov E. Direct cortical control of muscle activation in voluntary arm movements: a model. *Nature Neuroscience*, 3: 391–398, 2000.

Weinrich M and Wise SP. The premotor cortex of the monkey. *Journal of Neuroscience*, 2: 1329–1345, 1982.